REVISTA DE LA UNIÓN MATEMÁTICA ARGENTINA
Vol. 64, No. 2, 2023, Pages 487–510
Published online: August 29, 2023
https://doi.org/10.33044/revuma.3067

MATHEMATICAL MODEL FOR THE AQUATIC STAGE OF *AEDES AEGYPTI* CONSIDERING VARIABLE EGG-HATCHING RATE AND INTER-SPECIFIC COMPETITION BETWEEN LARVAL STAGES

TISHBE PILARH HERRERA-RAMÍREZ, ANDRÉS FRAGUELA-COLLAR, JORGE VELÁZQUEZ-CASTRO, AND CARLOS ANTONIO ABELLA-MEDRANO

Abstract. Mosquito-borne diseases like dengue, Zika, and chikungunya, carried by *Aedes aegypti* mosquitoes, pose significant health threats. Controlling these diseases primarily involves reducing mosquito populations. Current approaches rely on simplistic measures to decide on actions like mosquito fogging or larval control. Adult mosquito numbers are often estimated from aquatic populations due to easier counting. While these methods have provided some assistance, there's a need for improvement. Existing risk and population models overlook the various developmental stages of *Aedes aegypti* and their complex interactions. In this work, several mathematical models for the life cycle of the *Aedes aegypti* in its aquatic phase are proposed. They consider the different aquatic developmental stages and differ in how the competition between the stages occurs. Then, all the models are discriminated against experimental data to select the one with the best predictive power. The chosen model will help estimate the adult mosquito population with a greater degree of precision as well as when they will emerge. It will also help design better control strategies and better risk indices.

1. Introduction

The different dengue serotypes and the chikungunya and the Zika viruses are transmitted by the bite of an infected *Aedes aegypti* mosquito. The treatment of these diseases is not always effective, and there is currently no developed vaccination [5, 10]. The main strategies to prevent these diseases are the control of the transmitting vector and avoiding the human-vector contact [9, 5, 21]. During entomological surveillance programs, different indices have been defined to know if the number of mosquitoes remains below a threshold to avoid reinfections [23]. Historically, these programs have focused on measuring immature mosquito populations, due to the complexity of counting and capturing adult mosquitoes. On the

2020 *Mathematics Subject Classification.* 92D25, 92D30, 37N25.
Key words and phrases. Aedes aegypti life cycle, carrying capacity, hatchery productivity, mathematical modeling, larval stages, pupae, interspecific competition.

other hand, immature mosquitoes are in an aquatic phase; thus, their count reduces to the study of containers with water [15]. The most widely used indices are the Stegomyia indices (house index, container index, and Breteau index), which determine the percentage of houses and containers in which eggs, larvae, or pupae are detected [21]. These indices have been used to verify the effect of climate changes on mosquito populations [26], and also they are indicators of vector prevalence [24]. However, in 1999 the World Health Organization recognized that despite having some operational value to measuring the entomological impact in control interventions, they do not replace an actual estimation of the abundance of vectors at evaluating the risk in the transmission of dengue [18]. Thus, an increasing interest in developing measurement techniques and estimating the density of vectors has arisen. In particular, several studies have empirically evaluated the vector productivity of certain types of containers [4, 6, 2]. However, these experimental studies have not been integrated into a description of the dynamics of the mosquito's life cycle. On the other hand, epidemiological models of vector-borne diseases usually make simplifying assumptions about the life cycle of the mosquito [27, 11, 22]. The aquatic stages of the mosquito are reduced to a single parameter that represents the maximal production of mosquitoes in the region [20, 3] or, in some other cases, the carrying capacity [22].

In this article, we propose different mathematical models for the life cycle of the immature *Aedes aegypti* mosquito and compare their predictive power against experimental data. In this way, we can select the model that best fits the experimental data. The proposed models are based on reported entomological assumptions, and they are tested in the following order. In the first model, we test the common assumption of constant transition rates between stages of the life cycle [7, 29, 14]. In the second model, we evaluate the importance of the egg-hatching rate mediated by the hatchery density [13, 16]. Then, we study the effects of age-dependent hatching of eggs [28, 13] in the mosquito's life cycle. Next, we analyze the importance of competition of the larvae over the hatching. Finally, we explore a more complex schema of competition. There have been observations that not only the egg development but also the larval development may depend on the density of the system [19, 3, 16, 17]; therefore, in the last model, this competition is taken into account.

The model with more predictive power can be used in conjunction with epidemiological models of diseases transmitted by the *Aedes aegypti* and thus improve the prediction and evaluation of control strategies. In particular, it will be possible to compare different types of control at the aquatic stage; for example, the efficiency of a larvicide against biological control and elimination of breeding sites. Furthermore, the consideration of all developmental stages of the mosquito leads to a better prediction of the delay between the change in environmental factors like temperature and the risk of an outbreak. The improved descriptive power of the chosen model will bring about better strategies and a faster response in case of outbreak risk due to its dynamical description of the mosquito's life cycle.

Natural extensions can be made to this analysis, like considering broad geographical regions employing socio-economic factors. For example, the need for water storage and human population in different areas are relevant factors of regional hatchery productivity [9].

2. The models

The proposed models consider all the immature stages (eggs, larvae with four instars, and pupae) and the competition between these stages.

The following observation describes the notation that will be used.

Observation 2.1. The number of eggs introduced into the system per day is denoted by H. The pupae population is denoted by $p(t)$, and the eggs population by $h(t)$; $\tau_{0\,1}$ denotes the transition rate from egg to the first larvae instar, $\tau_{r\,r+1}$ represents the transition rate from the r-th to the $(r+1)$-th larvae instar, and $\tau_{5\,6}$ is the transition rate from pupae to adult mosquito. The mortality rate of eggs is denoted by μ_0, μ_r represents the mortality rate of the r-th larvae instar, and μ_5 the mortality rate of pupae. Thus $\tau_{0\,1}$ is the hatching rate, $\tau_{4\,5}$ is the pupation rate, and $\tau_{5\,6}$ is the rate of conversion from pupae to mosquitoes in adult stage.

The following conventions will let us simplify the notation: $\alpha_{i\,j} = \mu_i + \tau_{i\,j}$, $\tau = \tau_{1\,2}\tau_{2\,3}\tau_{3\,4}\tau_{4\,5}$, $\beta_{i\,j} = (\alpha_{i\,i+1})(\alpha_{i+1\,i+2})\dots(\alpha_{j-1\,j})$.

2.1. **Constant rates model.** A common assumption about the transition rates between stages of the mosquito's life cycle is to take them as constant [7, 29, 14]. We will analyze this basic model without competition between larvae instars, which is described by the following system of ordinary differential equations:

$$\begin{aligned}
\frac{dh}{dt} &= H - \mu_0 h - \tau_{0\,1} h,\\
\frac{dl_1}{dt} &= \tau_{0\,1} h - \mu_1 l_1 - \tau_{1\,2} l_1,\\
\frac{dl_2}{dt} &= \tau_{1\,2} l_1 - \mu_2 l_2 - \tau_{2\,3} l_2,\\
\frac{dl_3}{dt} &= \tau_{2\,3} l_2 - \mu_3 l_3 - \tau_{3\,4} l_3,\\
\frac{dl_4}{dt} &= \tau_{3\,4} l_3 - \mu_4 l_4 - \tau_{4\,5} l_4,\\
\frac{dp}{dt} &= \tau_{4\,5} l_4 - \mu_5 p - \tau_{5\,6} p.
\end{aligned} \tag{2.1}$$

The dependent variables of this model represent populations; thus, to have a biological sense, each variable must be non-negative at every instant of time. The biological sense set is then defined as

$$\Omega_1 = \{(h, l_1, l_2, l_3, l_4, p) \in \mathbb{R}^6_+ : l_1 + l_2 + l_3 + l_4 + p > 0 \text{ for } t > 0\},$$

where $\mathbb{R}^6_+$ denotes the set of vectors from $\mathbb{R}^6$ with non-negative values.

The following lemma will be needed to guarantee that the solution of (2.1) remains within the region of biological interest if initial conditions are taken in this region.

Lemma 2.2. *If $\mathcal{A}(t)$ and $\mathcal{B}(t)$ are continuous real functions defined on $[0,\infty)$, with $\mathcal{A}(t) \geq 0$, then every solution $x(t)$ of the first-order linear differential equation*

$$\frac{dx(t)}{dt} = \mathcal{A}(t) + \mathcal{B}(t)x(t)$$

with non-negative initial condition $(x(0) \geq 0)$ stays non-negative for all $t > 0$ $(x(t) \geq 0)$.

Moreover, if (t_0, t_1) is an open interval with $t_0 \geq 0$ where $\mathcal{A}(t)$ vanishes just in a finite number of points, then the solution $x(t)$ stays strictly positive on $(t_0, t_1]$.

Proof. For every $t_0 \geq 0$, if $B(t)$ is a primitive of $\mathcal{B}$ such that $B(0) = 0$ and $t \geq t_0$, then

$$x(t) = x(t_0)e^{B(t)} + e^{B(t)} \int_{t_0}^{t} \mathcal{A}(u)e^{-B(u)}\, du.$$

The first statement is deduced from the previous expression when $t_0 = 0$ and taking into account that both addends on the right-hand side expression are non-negative. The second statement is obtained directly from that expression where the integral term is strictly positive for $t \in (t_0, t_1]$. □

Theorem 2.3. *For the model given in (2.1), if the initial conditions are such that $h(0) \geq 0$, $l_1(0) \geq 0$, $l_2(0) \geq 0$, $l_3(0) \geq 0$, $l_4(0) \geq 0$, and $p(0) \geq 0$, then the solution will be strictly positive for $t > 0$.*

Proof. Note that the first equation of (2.1) decouples from the rest of the equations, and its solution is expressed by

$$h(t) = h(0)e^{-(\mu_0+\tau_{0\,1})t} + \frac{H}{\mu_0 + \tau_{0\,1}}\left(1 - e^{-(\mu_0+\tau_{0\,1})t}\right),$$

so $h(t)$ is strictly positive for $t > 0$, as long as $h(0) \geq 0$.

If we substitute the previous expression of $h(t)$ on the $l_1(t)$ equation and apply the second part of Lemma 2.2 setting $\mathcal{A}(t) = \tau_{0\,1}h(t)$ and $\mathcal{B}(t) = -(\mu_1 + \tau_{1\,2})$, it is concluded that $l_1(t) > 0$ for all $t > 0$. Repeating the same reasoning consecutively for $l_2(t)$, $l_3(t)$, $l_4(t)$ and $p(t)$, the theorem is proved. □

On the other hand, the Jacobian matrix of the system (2.1) is given by

$$\begin{bmatrix} -\alpha_{0\,1} & 0 & 0 & 0 & 0 & 0 \\ 0 & -\alpha_{1\,2} & 0 & 0 & 0 & 0 \\ 0 & \tau_{1\,2} & -\alpha_{2\,3} & 0 & 0 & 0 \\ 0 & 0 & \tau_{2\,3} & -\alpha_{3\,4} & 0 & 0 \\ 0 & 0 & 0 & \tau_{3\,4} & -\alpha_{4\,5} & 0 \\ 0 & 0 & 0 & 0 & \tau_{4\,5} & -\alpha_{5\,6} \end{bmatrix}$$

and its eigenvalues are

$$\lambda_r = -\alpha_{r\,r+1} = -(\mu_r + \tau_{r\,r+1}) < 0, \quad \text{with } r = 1, 2, 3, 4, 5, 6,$$

thus we can confirm that the only stationary value of the system (2.2) is stable and has a biological sense.

2.2. **Logistic saturation model.** Some observations have suggested that the hatching rate of eggs may be mediated by the density of the hatchery [13, 16]. In the next model we will take into account this competition for resources by means of a logistic term $\left(1-\frac{a(t)}{C_1}\right)$, where $a(t)$ corresponds to all individuals at the system, that is, $a(t)=l_1(t)+l_2(t)+l_3(t)+l_4(t)+p(t)$, and C_1 represents the carrying capacity. We will call $\left(1-\frac{a(t)}{C_1}\right)$ the *saturation term*. Thus, the per capita rate of hatching will be $\tau_{0\,1}\left(1-\frac{a(t)}{C_1}\right)$ and the total number of larvae generated by eggs per day is $\tau_{0\,1}h(t)\left(1-\frac{a(t)}{C_1}\right)$.

This model is represented by the following system of differential equations:

$$\begin{aligned}
\frac{dh}{dt} &= H-\mu_0 h-\tau_{0\,1}h\left(1-\frac{a}{C_1}\right),\\
\frac{dl_1}{dt} &= \tau_{0\,1}h\left(1-\frac{a}{C_1}\right)-\mu_1 l_1-\tau_{1\,2}l_1,\\
\frac{dl_2}{dt} &= \tau_{1\,2}l_1-\mu_2 l_2-\tau_{2\,3}l_2,\\
\frac{dl_3}{dt} &= \tau_{2\,3}l_2-\mu_3 l_3-\tau_{3\,4}l_3,\\
\frac{dl_4}{dt} &= \tau_{3\,4}l_3-\mu_4 l_4-\tau_{4\,5}l_4,\\
\frac{dp}{dt} &= \tau_{4\,5}l_4-\mu_5 p-\tau_{5\,6}p.
\end{aligned} \tag{2.2}$$

Due to its biological meaning, the hatching rate $\tau_{0\,1}\left(1-\frac{a(t)}{C_1}\right)$ should be non-negative. Thus, in addition to the positivity of the variables, the total number of specimens of all stages a must not exceed the carrying capacity. That means that $a(t)\leq C_1$ for all t. Therefore, we define the set of biological interest as

$$\Omega_2=\{(h,l_1,l_2,l_3,l_4,p)\in\mathbb{R}^6_+ : C_1\geq a>0\}.$$

Theorem 2.4. *If the initial conditions at $t=0$ of model (2.2) are in $\Omega_2\subset\mathbb{R}^6$, then its solution is in the topological interior of Ω_2 for all $t>0$.*

We show the proof of this theorem in the Appendix.

The system (2.2) has two stationary points given by

$$\begin{aligned} h^* &= \frac{H}{\mu_0} - \frac{\beta_{1\,6}}{\tau\mu_0}p^*, \\ l_1^* &= \frac{\beta_{2\,6}}{\tau}p^*, \\ l_2^* &= \frac{\beta_{3\,6}\tau_{1\,2}}{\tau}p^*, \\ l_3^* &= \frac{\beta_{4\,6}\tau_{1\,2}\tau_{2\,3}}{\tau}p^*, \\ l_4^* &= \frac{\beta_{5\,6}\tau_{1\,2}\tau_{2\,3}\tau_{3\,4}}{\tau}p^*, \end{aligned} \tag{2.3}$$

and

$$p^* = \frac{(\varphi C_1 + \psi H) \pm \sqrt{(\varphi C_1 + \psi H)^2 - 4\gamma H C_1}}{2}, \tag{2.4}$$

where $\gamma = \frac{\tau}{\beta_{1\,6}K_a}$, $\varphi = \frac{\mu_0+\tau_{0\,1}}{K_a\tau_{0\,1}}$ and $\psi = \frac{\tau}{\beta_{1\,6}}$. It also will be useful to notice that $a^* = K_a p^*$, with $a^* = l_1^* + l_2^* + l_3^* + l_4^* + p^*$ and

$$K_a := \left[\frac{\beta_{2\,6} + \beta_{3\,6}\tau_{1\,2} + \beta_{4\,6}\tau_{1\,2}\tau_{2\,3} + \beta_{5\,6}\tau_{1\,2}\tau_{2\,3}\tau_{3\,4}}{\tau} + 1\right].$$

If in (2.4) we write the discriminant $(\varphi C_1+\psi H)^2-4\gamma H C_1$ as $\left(\left(1 - \frac{\mu_0}{\tau_{0\,1}}\right)\frac{C_1}{K_a} + \psi H\right)^2 - 4\psi H\frac{C_1}{k_a}$ and expand this expression as a quadratic polynomial of the variable $\frac{C_1}{K_a}$, we have that it is equal to

$$\left(\frac{C}{K_a} - \psi H\right)^2 + \frac{\mu_0}{\tau_{0\,1}}\frac{C}{K_a}\left(\left(2 + \frac{\mu_0}{\tau_{0\,1}}\right)\frac{C}{K_a} + 2\psi H\right),$$

which is a strictly positive quantity. From the above it follows that the two values p^{*+} and p^{*-}, given by (2.4), are real, strictly positive and different.

On the other hand, for the equilibrium point p^*, given by expressions (2.3) and (2.4), to make biological sense it is necessary that $H - \frac{\beta_{1\,6}}{\tau}p^* > 0$ and $1 - \frac{a^*}{C_1} > 0$, which is equivalent to

$$p^* < \psi H$$

and

$$p^* < \frac{C_1}{K_a}.$$

In what follows, we will denote by p^{*+} and p^{*-} the values of p^* corresponding to the $+$ and $-$ signs, respectively, in the expression (2.4).

Theorem 2.5. *For all positive H and C_1, the following estimates are fulfilled:*

$$p^{*-} < \min\left\{\psi H, \frac{C_1}{K_a}\right\} \leq \max\left\{\psi H, \frac{C_1}{K_a}\right\} < p^{*+};$$

more precisely, if $\varphi C_1 - \psi H < 0$, we have

$$p^{*-} < \frac{C_1}{K_a} < \psi H < p^{*+}.$$

We show the proof of this theorem in the Appendix.

The previous theorem shows that only the equilibrium state corresponding to p^{*-} makes biological sense.

In the following theorem we will see that this equilibrium state is also stable and the equilibrium state corresponding to p^{*+} is always unstable.

Let us consider the Jacobian matrix of the system (2.2) evaluated at the stationary point, given by

$$A = \begin{bmatrix} -\mu_0 - \tau_{0\,1} + \frac{\tau_{0\,1}}{C_1}a^* & \frac{\tau_{0\,1}}{C_1}h^* & \frac{\tau_{0\,1}}{C_1}h^* & \frac{\tau_{0\,1}}{C_1}h^* & \frac{\tau_{0\,1}}{C_1}h^* & \frac{\tau_{0\,1}}{C_1}h^* \\ \frac{\tau_{0\,1}}{C_1}(C_1 - a^*) & -(\frac{\tau_{0\,1}}{C_1}h^* + \alpha_{1\,2}) & \frac{\tau_{0\,1}}{C_1}h^* & \frac{\tau_{0\,1}}{C_1}h^* & \frac{\tau_{0\,1}}{C_1}h^* & \frac{\tau_{0\,1}}{C_1}h^* \\ 0 & \tau_{1\,2} & -\alpha_{2\,3} & 0 & 0 & 0 \\ 0 & 0 & \tau_{2\,3} & -\alpha_{3\,4} & 0 & 0 \\ 0 & 0 & 0 & \tau_{3\,4} & -\alpha_{4\,5} & 0 \\ 0 & 0 & 0 & 0 & \tau_{4\,5} & -\alpha_{5\,6} \end{bmatrix},$$

where h^* and a^* correspond to the stationary states. In order to analyze the stability of the stationary points we study the roots of its characteristic polynomial

$$\det(A - \lambda I) = P(\lambda) + Q(\lambda),$$

where

$$P(\lambda) = (\lambda + \alpha_{2\,3})(\lambda + \alpha_{3\,4})(\lambda + \alpha_{4\,5})(\lambda + \alpha_{5\,6})P_1(\lambda)$$

and

$$Q(\lambda) = \tau_{1\,2}\frac{\tau_{0\,1}h^*}{C_1}\left(\mu_0 + 2\tau_{0\,1}\left(1 - \frac{a^*}{C_1}\right) + \lambda\right)Q_1(\lambda),$$

with

$$P_1(\lambda) = \left[\left(\mu_0 + \tau_{0\,1}\left(1 - \frac{a^*}{C_1}\right) + \lambda\right)\left(\frac{\tau_{0\,1}h}{C_1} + \alpha_{1\,2} + \lambda\right) - \tau_{0\,1}^2\left(1 - \frac{a^*}{C_1}\right)\left(\frac{h^*}{C_1}\right)\right]$$

and

$$Q_1(\lambda) = (\lambda + \alpha_{5\,6})[(\lambda + \alpha_{4\,5})(\lambda + \alpha_{3\,4} + \tau_{2\,3}) + \tau_{2\,3}\tau_{3\,4}] + \tau_{2\,3}\tau_{3\,4}\tau_{4\,5}.$$

Theorem 2.6. *For any strictly positive value of the parameter H, a value $C_1^0 > 0$ can be found, depending on H and the rest of the parameters of model* (2.2)*, such that, for any $C_1 \geq C_1^0$, the equilibrium point corresponding to p^{*-} is stable, while the one corresponding to p^{*+} is always unstable.*

We show the proof of this theorem in the Appendix.

Note that the previous theorem tells us that, although the equilibrium state corresponding to p^{*-} always makes biological sense for any value of the parameter C_1, it is not always stable, except for large values of C_1. The numerical criterion for the choice of C_1 must take into account the compromise between the best possible fit to the experimental data and the stability of the equilibrium state with a biological sense. That is, C_1 must be chosen in such a way that it is the smallest possible positive value that allows the data to be fitted and, at the same time,

large enough so that the stationary solution corresponding to p^{*-} is stable, which is equivalent to the polynomial $P(\lambda) + Q(\lambda)$ having all its roots with a negative real part.

Ensuring the biological validity of the equilibrium state guarantees the convergence to equilibrium for each larval stage and pupae. This alignment with numerical experiments corresponds to the model's predictions of observable outcomes.

Theorem 2.6 shows us that, if model (2.2) describes the dynamics of the *Aedes aegypti* mosquito in the aquatic state, we should observe that after a certain time the populations of larvae and pupae oscillate regularly around the stationary values given in (2.3) when in (2.4) we consider p^{*-}. However, this behavior is not observed, as we will see later when comparing with the experimental data.

The foregoing indicates that it is necessary to incorporate more biological information into the models so that their solutions fit more closely the experimental data. As we have already mentioned, the two models studied above correspond to the assumption that all the transitions are constants. However, in works such as [28, 13] it is mentioned that the hatching rate could have an erratic or non-constant behavior. This is the next assumption that we will take into consideration to improve the model.

2.3. **A model with variable hatching rate.** In [28, 13] it is mentioned that the hatching rate is not always constant. The non-regularity of the hatching rate can be a consequence of the age-dependent hatching of eggs. In the following model, we will consider that the hatching depends on each egg's time in the system. This age dependence may lead to a variable fraction of eggs hatching per day. To introduce this idea, we use an age model for the eggs population, and we couple it with the dynamics of the rest of the populations.

The population of eggs is now described by a two-variable function $\hat{h}(x,t)$, where t represents the time and x the age of the eggs. It is worth noticing that we refer to the age as the time elapsed since a particular egg was introduced into the system. The age-dependent hatching rate is denoted by $\tau(x)$.

The following system describes the proposed model:

$$\begin{aligned}
\frac{\partial \hat{h}}{\partial t} + \frac{\partial \hat{h}}{\partial x} &= -(\mu_0 + \tau(x))\hat{h} \\
\hat{h}(0,t) &= B(t) = H \\
\frac{dl_1}{dt} &= \int_0^\infty \tau(x)\hat{h}(x,t)\,dx - \mu_1 l_1 - \tau_{1\,2} l_1 \\
\frac{dl_2}{dt} &= \tau_{1\,2} l_1 - \mu_2 l_2 - \tau_{2\,3} l_2 \\
\frac{dl_3}{dt} &= \tau_{2\,3} l_2 - \mu_3 l_3 - \tau_{3\,4} l_3 \\
\frac{dl_4}{dt} &= \tau_{3\,4} l_3 - \mu_4 l_4 - \tau_{4\,5} l_4 \\
\frac{dp}{dt} &= \tau_{4\,5} l_4 - \mu_5 p - \tau_{5\,6} p.
\end{aligned}$$

Even if $B(t)$ can, in general, depend on time, we will set $B(t) = H$, a constant. This corresponds to assuming that the rate at which the eggs are introduced to the system is constant.

We notice that the first equation is not coupled with the rest of the system; thus, it is possible to solve it first. Using the method of characteristics, the solution of that equation is

$$\hat{h}(x,t) = \begin{cases} B(t-x)e^{-\mu_0 x}e^{\int_0^x \tau(z)\,dz} & \text{for } x < t, \\ 0 & \text{otherwise.} \end{cases}$$

Experimental results [28] have shown that all eggs hatch within the first 10 days, thus the relation $\sum_0^{10} \hat{\tau}(r) = 1$ is fulfilled, where $\hat{\tau}(r)$ represents the fraction of eggs that hatch at age r. Furthermore, if $B(r)$ represents the eggs that were introduced r time ago, the hatching rate is given by

$$\tau(x) = \sum_{r=0}^{x} \frac{\hat{\tau}(r)}{r} B(r) = H \sum_{r=0}^{x} \frac{\hat{\tau}(r)}{r}.$$

In addition to this, since $\hat{\tau}(x) = 0$ for $x \geq 10$, we have $\sum_0^x \frac{\hat{\tau}(r)}{r} = \sum_0^{10} \frac{\hat{\tau}(r)}{r}$. Thus, we notice that after day 10, the population hatching rate $\tau(x)$ keeps constant.

This particular behavior allows us to propose an effective model that will describe the populations from day 10 onward by defining $\tau_e = \tau(x)$ for $x \geq 10$:

$$\begin{aligned} \frac{dl_1}{dt} &= H\tau_e - \mu_1 l_1 - \tau_{1\,2} l_1 \\ \frac{dl_2}{dt} &= \tau_{1\,2} l_1 - \mu_2 l_2 - \tau_{2\,3} l_2 \\ \frac{dl_4}{dt} &= \tau_{3\,4} l_3 - \mu_4 l_4 - \tau_{4\,5} l_4 \\ \frac{dp}{dt} &= \tau_{4\,5} l_4 - \mu_5 p - \tau_{5\,6} p, \end{aligned} \tag{2.5}$$

where τ_e is the effective hatching rate. The model (2.5) represents a system where a constant number of eggs are deposited each day. It is possible to prove that this linear system is stable.

2.4. **Models with effective hatching rate and competition.** Now four different models are proposed to identify the importance of competition of the different instars on the hatching. The models are based on (2.5), and a general logistic competition term $\left(1 - \frac{L}{C}\right)$ is introduced multiplying the hatching term. The proposed

models are described by the following system of differential equations:

$$\begin{aligned}
\frac{dl_1}{dt} &= H\tau_e\left(1-\frac{L}{C}\right)-\mu_1 l_1-\tau_{1\,2}l_1\\
\frac{dl_2}{dt} &= \tau_{1\,2}l_1-\mu_2 l_2-\tau_{2\,3}l_2\\
\frac{dl_3}{dt} &= \tau_{2\,3}l_2-\mu_3 l_3-\tau_{3\,4}l_3\\
\frac{dl_4}{dt} &= \tau_{3\,4}l_3-\mu_4 l_4-\tau_{4\,5}l_4\\
\frac{dp}{dt} &= \tau_{4\,5}l_4-\mu_5 p-\tau_{5\,6}p.
\end{aligned} \tag{2.6}$$

In each model, L and C represent a different competition. So in order to evaluate the importance of the competition exerted from the different instars, we first assume

$$L=l_1,\ \text{thus}\ \left(1-\frac{l_1}{C_2}\right); \tag{2.7}$$

then we set

$$L=l_1+l_2,\ \text{thus}\ \left(1-\frac{l_1+l_2}{C_3}\right); \tag{2.8}$$

then

$$L=l_1+l_2+l_3,\ \text{thus}\ \left(1-\frac{l_1+l_2+l_3}{C_4}\right), \tag{2.9}$$

and finally

$$L=l_1+l_2+l_3+l_4,\ \text{thus}\ \left(1-\frac{l_1+l_2+l_3+l_4}{C_5}\right). \tag{2.10}$$

The unique stationary state of model (2.7) is given by

$$(l_1^*,l_2^*,l_3^*,l_4^*,p^*)=\left(\frac{C_2\,H\tau_e}{H\tau_e+C_2\,\alpha_{1\,2}},\ \frac{\tau_{1\,2}}{\alpha_{2\,3}}l_1^*,\ \frac{\tau_{2\,3}}{\alpha_{3\,4}}l_2^*,\ \frac{\tau_{3\,4}}{\alpha_{4\,5}}l_3^*,\ \frac{\tau_{4\,5}}{\alpha_{5\,6}}l_4^*\right),$$

while the unique stationary state of model (2.8) is

$$\begin{aligned}
&(l_1^*,l_2^*,l_3^*,l_4^*,p^*)\\
&\quad=\left(\frac{C_3\,H\tau_e\alpha_{2\,3}}{H\tau_e(\alpha_{2\,3}+\tau_{1\,2})+C_3\,\alpha_{1\,2}\alpha_{2\,3}},\ \frac{\tau_{1\,2}}{\alpha_{2\,3}}l_1^*,\ \frac{\tau_{2\,3}}{\alpha_{3\,4}}l_2^*,\ \frac{\tau_{3\,4}}{\alpha_{4\,5}}l_3^*,\ \frac{\tau_{4\,5}}{\alpha_{5\,6}}l_4^*\right).
\end{aligned}$$

Model (2.9) has a unique stationary state given by

$$\begin{aligned}
(l_1^*,l_2^*,l_3^*,l_4^*,p^*)=\Bigg(&\frac{C_4\,H\tau_e\alpha_{2\,3}\alpha_{3\,4}}{H\tau_e(\alpha_{2\,3}\alpha_{3\,4}+\alpha_{3\,4}\tau_{1\,2}+\tau_{1\,2}\tau_{2\,3})+C_4\,\alpha_{1\,2}\alpha_{2\,3}\alpha_{3\,4}},\\
&\frac{\tau_{1\,2}}{\alpha_{2\,3}}l_1^*,\frac{\tau_{2\,3}}{\alpha_{3\,4}}l_2^*,\frac{\tau_{3\,4}}{\alpha_{4\,5}}l_3^*,\frac{\tau_{4\,5}}{\alpha_{5\,6}}l_4^*\Bigg),
\end{aligned}$$

and finally the unique stationary state of model (2.10) is

$$(l_1^*,l_2^*,l_3^*,l_4^*,p^*)=\left(\frac{C_5\,H\tau_e\alpha_{2\,3}\alpha_{3\,4}\alpha_{4\,5}}{H\tau_e\Gamma'+C_5\,\alpha_{1\,2}\alpha_{2\,3}\alpha_{3\,4}\alpha_{4\,5}},\ \frac{\tau_{1\,2}}{\alpha_{2\,3}}l_1^*;\ \frac{\tau_{2\,3}}{\alpha_{3\,4}}l_2^*,\ \frac{\tau_{3\,4}}{\alpha_{4\,5}}l_3^*,\ \frac{\tau_{4\,5}}{\alpha_{5\,6}}l_4^*\right),$$

where

$$\Gamma' = (\alpha_{2\,3}\alpha_{3\,4}\alpha_{4\,5} + \alpha_{4\,5}\alpha_{3\,4}\tau_{1\,2} + \alpha_{4\,5}\tau_{1\,2}\tau_{2\,3} + \tau_{1\,2}\tau_{2\,3}\tau_{3\,4}).$$

2.5. **A model with more general competition.** The previous models introduced the reduction of egg-hatching due to the competition for resources. In the following model, we explore a more complex schema of competition. There have been observations that not only egg development but also larval development may depend on the density of the system [19, 3, 16]. We take into account this dependency by introducing logistic transition rates between different instars. In particular, we assume that instars 3 and 4 exert the most relevant competition in the system. We can summarize our entomological assumptions as follows:

- Every day, a constant number of eggs enter the system.
- The mortality rates are constants.
- The hatching rate is variable, although in our case it corresponds to an effective rate from day 10 onward.
- Egg hatching is affected by the number of first instar larvae.
- The third and fourth instar affect logistically the larval transition.

The last assumption considers that the fourth instar can delay its development for several weeks due to lack of food [17] and identifies the third and fourth instar as the most significant competitors against other larvae.

The proposed model is described by

$$\begin{aligned}
\frac{dl_1}{dt} &= H\tau_e\left(1-\frac{l_1}{C_6}\right) - \mu_1 l_1 - \left(1-\frac{l_3}{C_7}\right)\left(1-\frac{l_4}{C_8}\right)\tau_{1\,2}l_1,\\
\frac{dl_2}{dt} &= \left(1-\frac{l_3}{C_7}\right)\left(1-\frac{l_4}{C_8}\right)\tau_{1\,2}l_1 - \mu_2 l_2 - \left(1-\frac{l_3}{C_7}\right)\left(1-\frac{l_4}{C_8}\right)\tau_{2\,3}l_2,\\
\frac{dl_3}{dt} &= \left(1-\frac{l_3}{C_7}\right)\left(1-\frac{l_4}{C_8}\right)\tau_{2\,3}l_2 - \mu_3 l_3 - \left(1-\frac{l_3}{C_7}\right)\left(1-\frac{l_4}{C_8}\right)\tau_{3\,4}l_3,\\
\frac{dl_4}{dt} &= \left(1-\frac{l_3}{C_7}\right)\left(1-\frac{l_4}{C_8}\right)\tau_{3\,4}l_3 - \mu_4 l_4 - \tau_{4\,5}\left(1-\frac{l_4}{C_8}\right)l_4,\\
\frac{dp}{dt} &= \tau_{4\,5}\left(1-\frac{l_4}{C_8}\right)l_4 - \mu_5 p - \tau_{5\,6}p.
\end{aligned} \tag{2.11}$$

Due to the complexity of the model, it was not analyzed analytically, but the numerical solutions were compared directly with the experimental data.

3. Model parameters

Table 1 shows the values of the parameters that were used to obtain the numerical solutions of the models. The values were taken from specialized literature in entomology. The information taken into account is the duration of each stage and the percentage of mortality. All parameters correspond to similar environmental conditions (25–30 °C, 70–80% RH). When necessary, the mortality rates were calculated as the inverse of the mean duration at the stage multiplied by the

percentage of mortality in that stage. In a similar way, the transition rates can be calculated from the survival percentages that are observed in experiments.

parameter	value	reference
$\tau_{0\,1}$	0.136	[8]
$\tau_{1\,2}$	0.508	[25]
$\tau_{2\,3}$	0.529	[25]
$\tau_{3\,4}$	0.095	[12]
$\tau_{4\,5}$	0.045	[12]
$\tau_{5\,6}$	0.410	[7]
μ_0	0.064	[17]
μ_1	0.339	[17]
μ_2	0.062	[17, 12]
μ_3	0.075	[17, 12]
μ_4	0.053	[17, 12]
μ_5	0.062	[17, 12]
τ_e	0.5046	[28]

TABLE 1. Values of parameters.

The values of C in the logistic terms of the model are not typically reported in the literature. Thus we performed a Markov chain Monte Carlo numerical analysis to find the C, with the greatest likelihood when comparing the model with the Rinconada experiment. The value obtained for C_1 was 73.0806. We proceeded in a similar way to estimate the best value for C in models represented by (2.6). For model (2.7) the best approximation to the data was given by $C_2 = 15.6894$. For model (2.8) we obtained the best fit with $C_3 = 28.707$, and for model (2.9) with $C_4 = 58.5359$. Finally, we set $C_5 = 80.6151$ in model (2.10) and $C_6 = 15.29$, $C_7 = 300.35$, $C_8 = 500.27$ in model (2.11).

4. Data acquisition

The data were taken in Rinconada, Veracruz, in Mexico. The experiment was carried out under the following environmental conditions: daily mean temperature of 25–30 °C, relative humidity of 70–80% with a photoperiod of 12:12. Three different types of polycarbonate containers were used. Each container was filled with 2 liters of water and 0.8 grams of food. In each container, 100 eggs were deposited each day for 25 days.

The dimensions of the containers were as follows:

- Type 1 containers: 30 cm × 25 cm with a depth of 5 cm.
- Type 2 containers: 28 cm × 20 cm with a depth of 15 cm.

- Type 3 containers: Circular containers with a diameter of 28 cm with a depth of 15 cm.

The populations in the containers were measured on the eleventh day of the experiment and every two days after that. In order not to disturb the dynamics during the measurements, there were eight containers of each type. One container was used for the measurements each day, but the others were not disturbed so that the dynamics could follow their natural path. Once a container was used for the measurements, it was eliminated from the experiment. The collected data corresponds to the number of larvae and pupae counted on that day. For each type of container, the measurement was performed twice. The six experiment instances (two for each container type) were conducted simultaneously to mitigate potential variations stemming from diverse environmental conditions. The mathematical models will be compared with the population mean of the six samples for each day.

5. Model simulations and results

We made numerical simulations of the proposed models and calculated the mean squared error (MSE) between the data points and each model's prediction.

The solution of model (2.1) is shown in Figure 1. Figure 2 shows the solution of model (2.2). The models given by (2.7), (2.8), (2.9) and (2.10) are compared in Figure 3. Finally, the numerical solution to the model with more general competition (2.11) can be seen in Figure 4.

Table 2 shows the MSE between the proposed models and the experimental data.

The MSE of the model that considers the logistic saturation on the hatching (2.2) is smaller than that of the simpler model (2.1), where competition is not taken into account. The smaller MSE for model (2.2) indicates that the hatching rate is reduced by lack of food and thus by the high density of larvae. It is worth noticing that eggs may accumulate in large quantities and hatch when most larvae become adult mosquitoes. The previously described phenomenon is a consequence of the low mortality rate of eggs and makes the population of *Aedes aegypti* very resilient in its aquatic stage.

Moreover, models (2.7), (2.8), (2.9) and (2.10) have better performance than the previous ones. The better performance of model (2.7) gives us further insight into the mosquito's life cycle, indicating that the first larvae instar is the primary factor of the hatching rate inhibition. On the other hand, model (2.11) has the best performance of all the studied models, showing that the competition between different instars also plays an important role.

6. Discussion

By comparing different models with experimental data, we found that a model that takes into account the competition between *Aedes aegypti* developmental stages better describes the experimental observations than a model that neglects these interactions. For example, model (2.11) can be used in the design and evaluation of vector control strategies as it gives a good description of the dynamics of

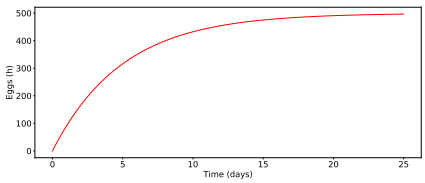

(a) Dynamics of eggs

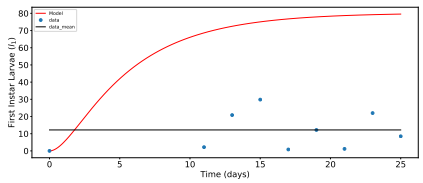

(b) Dynamics of first larvae population

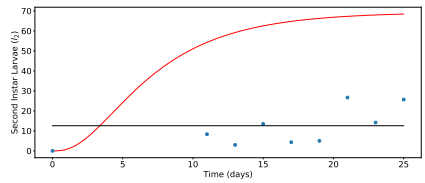

(c) Dynamics of second larvae population

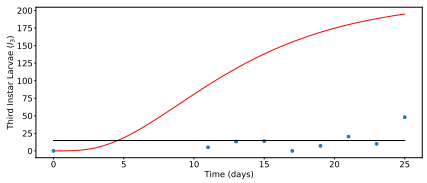

(d) Dynamics of third larvae population

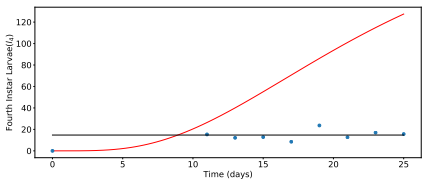

(e) Dynamics of fourth larvae population

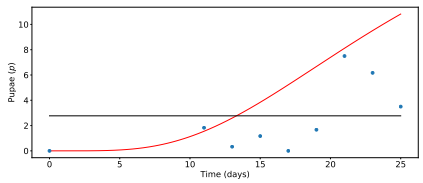

(f) Dynamics of pupae population

FIGURE 1. Dynamics by instar of the constant coefficient model (2.1).

Models	(2.1)	(2.2)	(2.7)	(2.8)	(2.9)	(2.10)	(2.11)
MSE	44974						
MSE, C_1= 73.08		122					
MSE, C_2=15.6894			68.60				
MSE, C_3=28.707				68.88			
MSE, C_4=58.535					77.99		
MSE, C_5=80.615						81.14	
MSE, C_6=15.29, C_7=300.3, C_8=500.27							65.23

TABLE 2. Comparison of models by mean squared error.

the mosquito's life cycle. This model can also be coupled with an epidemiological model to estimate the impact of the control measures of dengue, Zika, chikungunya, or any other disease transmitted by the *Aedes aegypti* mosquito. In contrast with other models of the mosquito's life cycle that have been used in epidemiology, the proposed model takes into account the different developmental stages of the vector, allowing a better timing between hatchery control and its effects on the

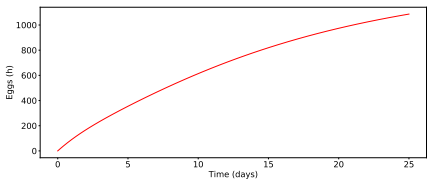

(a) Dynamics of eggs

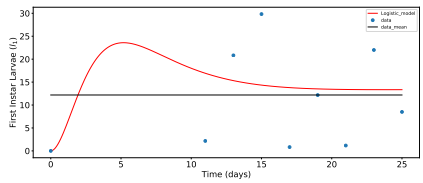

(b) Dynamics of first larvae population

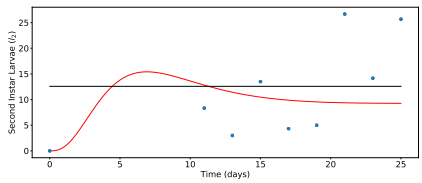

(c) Dynamics of second larvae population

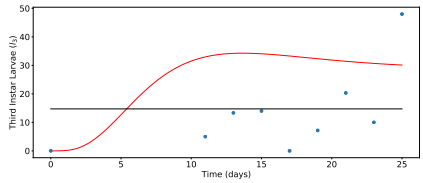

(d) Dynamics of third larvae population

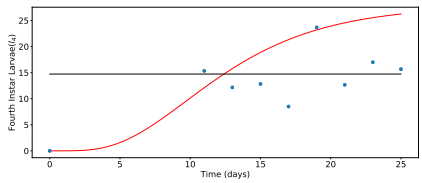

(e) Dynamics of fourth larvae population

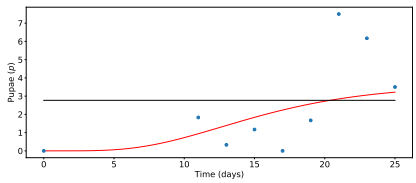

(f) Dynamics of pupae population

FIGURE 2. Dynamics by instar of model (2.2).

propagation of diseases. On the other hand, estimation of hatchery productivity is a fundamental task but not a trivial one. Usually, in order to quantify epidemic risk, the productivity of the hatcheries is substituted by simple empirical indices like the house index or the Breteau index. These indices give a poor description of the situation, being only descriptive but not predictive.

This study shows that the competition between different developmental stages of the *Aedes aegypti* is an important factor in estimating hatchery productivity. This better description of hatchery productivity will facilitate the development of more accurate risk indexes. These models can also be extended to include social factors like water supply to estimate the regional mosquito productivity in future works. The prediction of mosquito productivity in broad areas is important to predict outbreaks in extended geographical regions and in the description of the spatial propagation of the disease. Due to the aquatic nature of the hatcheries, it is expected that the population's need to store water will be one of the most relevant factors for mosquito production in a particular region. If there is a significant need to keep water in vessels due to the lack of tap water, then these vessels can become hatcheries.

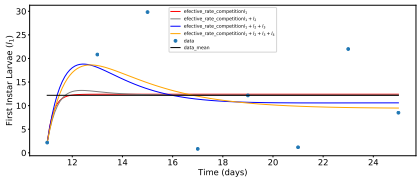

(a) Dynamics of first larvae population

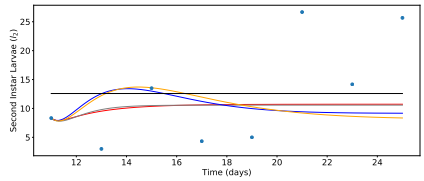

(b) Dynamics of second larvae population

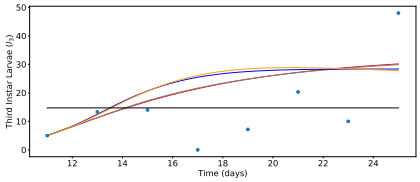

(c) Dynamics of third larvae population

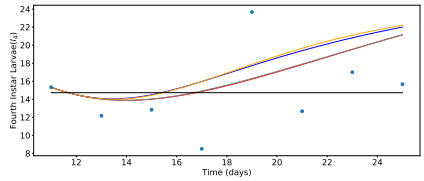

(d) Dynamics of fourth larvae population

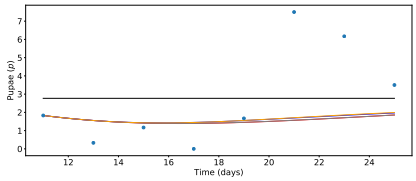

(e) Dynamics of pupae population

FIGURE 3. Dynamics by instar to the effective rate and logistics saturation about different models (2.7), (2.8),(2.9), (2.10).

7. APPENDIX

In this appendix we present the proofs of Theorems 2.4, 2.5 and 2.6.

Theorem 2.4 *If the initial conditions at $t = 0$ of model (2.2) are in $\Omega_2 \subset \mathbb{R}^6$, then its solution is in the topological interior of Ω_2 for all $t > 0$.*

Proof. We divide the proof in four parts.

First part. If we apply Lemma 2.2 to the first equation of (2.2), taking $\mathcal{A}(t) = H$ and $\mathcal{B}(t) = -\tau_{0\,1}\left(1 - \frac{a}{C_1}\right)$ regardless of the values of $a(t)$, we have that $h(t) > 0$ in $t > 0$. If $l_1(t)$ is non-negative and vanishes in just a finite number of points on (t_0, t_1), we conclude from Lemma 2.2 and the last four equations of (2.2) that $l_2(t)$, $l_3(t)$, $l_4(t)$ and $p(t)$ are strictly positive for all $t \in (t_0, t_1]$ for every open interval on $[0, \infty)$.

Second part. Now we consider the $l_1(t)$ equation in a neighborhood of $t = 0$ and show that there exists a neighborhood to the left of $t = 0$ where $l_1(t)$ is strictly positive. This is trivial if $l_1(0) > 0$. Suppose then that $l_1(0) = 0$.

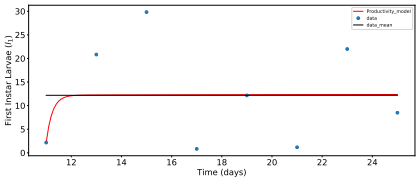

(a) Dynamics of first larvae population

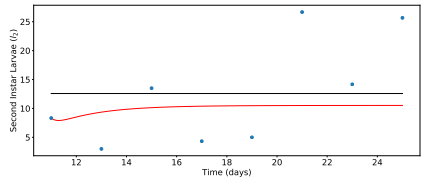

(b) Dynamics of second larvae population

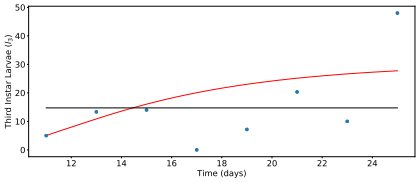

(c) Dynamics of third larvae population

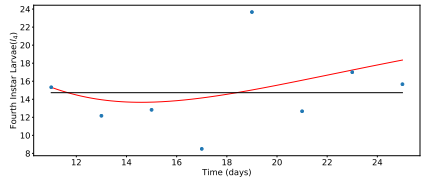

(d) Dynamics of fourth larvae population

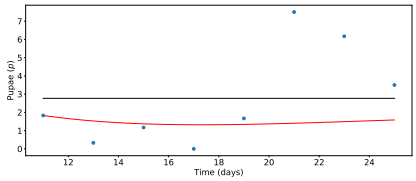

(e) Dynamics of pupae population

FIGURE 4. Dynamics by instar of model (2.11).

From the equation for $l_1(t)$ we get

$$\frac{dl_1(0)}{dt} = \tau_{0\,1} h(0) \left(1 - \frac{a(0)}{C_1}\right). \tag{7.1}$$

From (7.1) we have that if $h(0) > 0$ and $a(0) < C_1$, then $\frac{dl_1(0)}{dt} > 0$, so on a left neighborhood of $t = 0$ it would be true that $l_1(t) > 0$.

On the other hand, if we had $h(0) = 0$ or $a(0) = C_1$, then $\frac{dl_1(0)}{dt} = 0$. In this case we can have three possible combinations: $h(0) = 0$ with $a(0) < C_1$, $h(0) > 0$ with $a(0) = C_1$, or $h(0) = 0$ with $a(0) = C_1$.

Let us assume the first case, that is, when $h(0) = 0$ with $a(0) < C_1$. If we differentiate the $l_1(t)$ equation and evaluate the result at $t = 0$, we have

$$\frac{d^2 l_1}{dt^2}(0) = \tau_{0\,1} \frac{dh}{dt}(0) \left(1 - \frac{a(0)}{C_1}\right) - \frac{\tau_{0\,1}}{C_1} h(0) \frac{da}{dt}(0) - (\mu_1 + \tau_{1\,2}) \frac{dl_1}{dt}(0). \tag{7.2}$$

But from the equation for $h(t)$ evaluated at $t = 0$ we have $\frac{dh}{dt}(0) = H$ and then (7.2) is given by

$$\frac{d^2 l_1}{dt^2}(0) = \tau_{0\,1} H \left(1 - \frac{a(0)}{C_1}\right).$$

From the fact that $l_1(0) = 0$, $\frac{dl_1}{dt}(0) = 0$ and $\frac{d^2l_1}{dt^2}(0) > 0$, and using the second-order Taylor formula applied to $l_1(t)$ on the interval $[0, t]$ with t close enough to 0, we have $l_1(t) > 0$ for all t in a neighborhood to the right of $t = 0$.

In the second case, when $h(0) > 0$ and $a(0) = C_1$, from (7.2) we obtain

$$\frac{d^2l_1}{dt^2}(0) = -\frac{\tau_{0\,1}}{C_1}h(0)\frac{da}{dt}(0). \tag{7.3}$$

Adding the equations of $l_1(t)$, $l_2(t)$, $l_3(t)$, $l_4(t)$ and $p(t)$, from (2.2), we get

$$\frac{da}{dt} = \tau_{0\,1}h\left(1 - \frac{a}{C_1}\right) - (\mu_1 l_1 + \mu_2 l_2 + \mu_3 l_3 + \mu_4 l_4 + \mu_5 p + \tau_{5\,6}p). \tag{7.4}$$

If we now evaluate this equation at $t = 0$, then since $a(0) = C_1$ we have

$$\frac{da(0)}{dt} = -(\mu_1 l_1(0) + \mu_2 l_2(0) + \mu_3 l_3(0) + \mu_4 l_4(0) + \mu_5 p(0) + \tau_{5\,6}p(0)). \tag{7.5}$$

Nevertheless, we have assumed that the initial conditions belong to Ω_2 so all the numbers $l_1(0)$, $l_2(0)$, $l_3(0)$, $l_4(0)$ and $p(0)$ are non-negative and their sum is strictly positive, from which we can conclude that at least one of them is strictly positive. And since μ_1, μ_2, μ_3, μ_4, μ_5, $\tau_{5\,6}$ are strictly positive, the right-hand side of (7.5) is strictly negative and so $\frac{da(0)}{dt} < 0$.

Then from (7.3) it is concluded that in this case we also have $\frac{d^2l_1}{dt^2}(0) > 0$, and applying the same reasoning with Taylor's formula that we applied in the previous case, again we obtain $l_1(t) > 0$ in a neighborhood to the right of $t = 0$.

Finally, consider the third case, where $h(0) = 0$ and $a(0) = C_1$. In this case, from (7.2) we get $\frac{d^2l_1}{dt^2}(0) = 0$, but then if we differentiate twice the equation for $l_1(t)$ and evaluate the result at $t = 0$, we have

$$\begin{aligned}\frac{d^3l_1}{dt^3}(0) = \tau_{0\,1}&\left(\frac{d^2h(0)}{dt^2}\left(1 - \frac{a(0)}{C_1}\right) - \frac{2}{C_1}\frac{dh(0)}{dt}\frac{da(0)}{dt} - \frac{h(0)}{C_1}\frac{d^2a(0)}{dt^2}\right)\\ &- (\mu_1 + \tau_{1\,2})\frac{d^2l_1(0)}{dt^2},\end{aligned}$$

from which, using (7.4) and $\frac{dh(0)}{dt} = H$, we get that

$$\begin{aligned}\frac{d^3l_1}{dt^3}(0) &= -\frac{2}{C_1}\frac{dh(0)}{dt}\frac{da(0)}{dt}\\ &= \frac{2}{C_1}H(\mu_1 l_1(0) + \mu_2 l_2(0) + \mu_3 l_3(0) + \mu_4 l_4(0) + \mu_5 p(0) + \tau_{5\,6}p(0))\end{aligned}$$

and therefore $\frac{d^3l_1}{dt^3}(0) > 0$.

Subsequently, applying the third-order Taylor formula to $l_1(t)$ in a small neighborhood to the right of $t = 0$, we get $l_1(t) > 0$ for all t in that neighborhood.

As a conclusion of this second part, we get that if the initial conditions are in Ω_2, then $l_1(t) > 0$ for all t in a neighborhood to the right of $t = 0$.

Third part. If now we consider the preimage of the unitary set $\{0\}$, which is closed, we get that $l_1^{-1}\{0\}$ is a closed subset in $t \geq 0$ that at least contains 0 as an isolated point, which occurs if $l_1(0) = 0$ due to the final conclusion from the

second part of this proof. Then the closed set $l_1^{-1}\{0\} \setminus \{0\}$ could be the empty set, and $l_1(t)$ will be strictly positive for $t > 0$. Even so, the set $l_1^{-1}\{0\} \setminus \{0\}$ could be closed and non-empty, with a minimum at $t_0 > 0$. In this case, the point t_0 will be the lowest strictly positive real number such that $l_1(t_0) = 0$ and $l_1(t) > 0$ for all $t \in (0, t_0)$.

Next we will show that this situation is not possible and therefore if $l_1(0) \geq 0$ then $l_1(0) > 0$ for all $t > 0$.

Fourth part. Indeed, we start by showing that in the second case the functions $l_2(0)$, $l_3(0)$, $l_4(0)$ and $p(0)$ will get strictly positive in the semi-open interval $(0, t_0]$.

These results are obtained as consequences of Lemma 2.2: First for $l_2(t)$, taking $\mathcal{A}(t) = \tau_{1\,2} l_1(t)$ and $\mathcal{B} = -(\mu_2 + \tau_{2\,3})$; then for $l_3(t)$, taking $\mathcal{A}(t) = \tau_{2\,3} l_2(t)$ and $\mathcal{B} = -(\mu_3 + \tau_{3\,4})$; then for $l_4(t)$, taking $\mathcal{A}(t) = \tau_{3\,4} l_3(t)$ and $\mathcal{B} = -(\mu_4 + \tau_{4\,5})$; and finally for $p(t)$, taking $\mathcal{A}(t) = \tau_{4\,5} l_4(t)$ and $\mathcal{B} = -(\mu_5 + \tau_{5\,6})$.

On the other hand, it is easy to see that equation (7.4) is equivalent to

$$\frac{d}{dt}\left(1 - \frac{a(0)}{C_1}\right) = \frac{1}{C_1}(\mu_1 l_1 + \mu_2 l_2 + \mu_3 l_3 + \mu_4 l_4 + \mu_5 p + \tau_{5\,6} p) - \frac{\tau_{0\,1}}{C_1} h \left(1 - \frac{a(0)}{C_1}\right). \tag{7.6}$$

We will apply Lemma 2.2 to this equation, considering $\mathcal{A} = \frac{1}{C_1}(\mu_1 l_1 + \mu_2 l_2 + \mu_3 l_3 + \mu_4 l_4 + \mu_5 p + \tau_{5\,6} p)$ and $\mathcal{B} = \frac{\tau_{0\,1}}{C_1} h$. But, from the results of the third part and the beginning of this fourth part, it is concluded that $l_1(t)$, $l_2(t)$, $l_3(t)$, $l_4(t)$ and $p(t)$ are strictly positive on the interval $(0, t_0]$, and since μ_1, μ_2, μ_3, μ_4, μ_5, $\tau_{5\,6}$ are strictly positive too, $\mathcal{A} > 0$ for $t \in (0, t_0]$, and from Lemma 2.2 it is concluded that $1 - \frac{a(t)}{C_1} > 0$ on $(0, t_0]$, thus $a(t) < C_1$ on $(0, t_0]$.

If now we consider the equation for l_1 from the system (2.2) and evaluate it at t_0, from the fact that $l_1(t_0) = 0$ we get

$$\frac{dl_1(t_0)}{dt} = \tau_{0\,1} h(t_0) \left(1 - \frac{a(0)}{C_1}\right) > 0,$$

which contradicts our assumption, $l_1(t) > 0$ on $(0, t_0)$. Indeed, based on this last idea, we conclude that $\frac{dl_1(t_0)}{dt} \leq 0$.

Thus, the assumption that there exists a lowest value $t_0 > 0$ where $l_1(t_0) = 0$ is wrong, and therefore $l_1(t) > 0$ for all $t > 0$. But then, repeating the same reasoning from the beginning of this fourth part, we get that $l_2(t)$, $l_3(t)$, $l_4(t)$ and $p(t)$ are strictly positive for all $t > 0$, and by the reasoning just used with equation (7.6) we conclude that $a(t) < C_1$ for all $t > 0$.

Finally, from this conclusion, we can affirm that if the initial conditions of the system (2.2) are in Ω_2, the solution $(h(t), l_2(t), l_2(t), l_3(t), l_4(t), p(t))$ remains inside Ω_2 for all $t > 0$, that is, all its components are strictly positive and $a(t) < C_1$. □

Theorem 2.5 *For all positive H and C_1, the following estimates are fulfilled:*

$$p^{*-} < \min\left\{\psi H, \frac{C_1}{K_a}\right\} \leq \max\left\{\psi H, \frac{C_1}{K_a}\right\} < p^{*+}; \tag{7.7}$$

more precisely, if $\varphi C_1 - \psi H < 0$*, we have*

$$p^{*-} < \frac{C_1}{K_a} < \psi H < p^{*+}. \tag{7.8}$$

Proof. It is obvious that from (7.8) we get (7.7), in the case $\varphi C_1 - \psi H < 0$. Let us start by proving (7.8). Notice that, in this case, the inequality $\frac{C_1}{K_a} < \psi H$ is a consequence of $\frac{C_1}{K_a} < \varphi C_1 < \psi H$, and, therefore, it suffices to show that $p^{*-} < \frac{C_1}{K_a}$ and $p^{*+} > \psi H$. To see that $p^{*-} < \frac{C_1}{K_a}$, we consider the equality

$$2\left(p^{*-} - \frac{C_1}{K_a}\right) = \frac{\mu_0}{\tau_{0\,1}}\frac{C}{K_a} + \psi H - \frac{C_1}{K_a} - \sqrt{(\varphi C_1 + \psi H)^2 - 4\gamma H C_1}. \tag{7.9}$$

The right-hand side of (7.9) will be negative if and only if

$$\begin{aligned}\left(\frac{\mu_0}{\tau_{0\,1}}\frac{C}{K_a} + \psi H - \frac{C_1}{K_a}\right)^2 &- (\varphi C_1 + \psi H)^2 - 4\gamma H C_1 \\ &= \left((\varphi C_1 + \psi H) - 2\frac{C_1}{K_a}\right)^2 - (\varphi C_1 + \psi H)^2 - 4\gamma H C_1 \\ &= -4\frac{\mu_0}{\tau_{0\,1}}\frac{C_1^2}{K_a^2},\end{aligned}$$

which is evident, and this proves the inequality $p^{*-} < \frac{C}{K_a}$. To prove that $p^{*+} > \psi H$, we start from the equality

$$2(p^{*+} - \psi H) = \sqrt{(\varphi C_1 + \psi H)^2 - 4\gamma H C_1} + \varphi C_1 - \psi H. \tag{7.10}$$

From the fact that $\varphi C_1 - \psi H < 0$, it follows that (7.10) is positive if and only if $(\varphi C_1 + \psi H)^2 - 4\gamma H C_1 - (\varphi C_1 + \psi H)^2 = 4\frac{\mu_0}{\tau_{0\,1}}\frac{\psi}{K_a} H C_1$, which is obvious.

Let us now go on to prove inequalities (7.7) in the case $\varphi C_1 - \psi H \geq 0$. We will first show that, in this case, we have $p^{*-} < \psi H$. Indeed, from the equality

$$2(p^{*-} - \psi H) = (\varphi C_1 - \psi H) - \sqrt{(\varphi C_1 - \psi H)^2 - 4\gamma H C_1}$$

we have that the inequality is fulfilled if the following expression is negative:

$$(\varphi C_1 - \psi H)^2 - (\varphi C_1 - \psi H)^2 + 4\gamma H C_1 = -4\frac{\mu_0}{\tau_{0\,1}}\frac{\psi}{K_a} H C_1,$$

which is evident.

To show that $p^{*-} < \frac{C_1}{K_a}$ when $\varphi C_1 - \psi H \leq 0$, we will divide the proof into two subcases:

$$\varphi C_1 \geq \psi H \geq \frac{C_1}{K_a} \qquad \text{and} \qquad \varphi C_1 \geq \frac{C_1}{K_a} \geq \psi H. \tag{7.11}$$

In the first subcase, the proof made with (7.9) is repeated; in the second subcase, from (7.9) we have the inequality

$$2\left(p^{*+} - \frac{C_1}{K_a}\right) \leq \frac{\mu_0}{\tau_{0\,1}}\frac{C_1}{K_a} - \sqrt{(\varphi C_1 + \psi H)^2 - 4\gamma H C_1},$$

where the left-hand side is less than the right-hand side of equality (7.9), which is less than zero, and this allows us to conclude the result. In the case $\varphi C_1 - \psi H \leq 0$,

the right-hand side of (7.10) is greater than zero and then $p^{*+} > \psi H$. Let us finally prove that $p^{*+} > \frac{C_1}{k_a}$ when $\varphi C_1 - \psi H \geq 0$, and for this we will divide the proof into the two subcases (7.11).

In the first subcase, the proof is obtained directly from the equality

$$2\left(p^{*+} - \frac{C_1}{K_a}\right) = \frac{\mu_0}{\tau_{0\,1}}\frac{C_1}{K_a} + \left(\psi H - \frac{C_1}{K_a}\right) + \sqrt{(\varphi C_1 + \psi H)^2 - 4\gamma H C_1}. \quad (7.12)$$

In the second subcase, notice that from (7.12) we obtain the inequality

$$2\left(p^{*+} - \frac{C_1}{K_a}\right) \geq \left(\psi H - \frac{C_1}{K_a}\right) + \sqrt{(\varphi C_1 + \psi H)^2 - 4\gamma H C_1}, \quad (7.13)$$

and since $(\psi H - \frac{C_1}{K_a}) \leq 0$, the right-hand side of (7.13) will be positive if

$$(\varphi C_1 + \psi H)^2 - 4\gamma H C - \left(\psi H - \frac{C_1}{K_a}\right)^2 = \frac{\mu_0}{\tau_{0\,1}}\left(2 + \frac{\mu_0}{\tau_{0\,1}}\right)\frac{C_1^2}{K_a^2} + 2\psi H \frac{\mu_0}{\tau_{0\,1}}\frac{C_1^2}{K_a^2},$$

which is evident, and thus the proof of the theorem is concluded. □

Theorem 2.6 *For any strictly positive value of the parameter H, a value $C_1^0 > 0$ can be found, depending on H and the rest of the parameters of model* (2.2)*, such that, for any $C_1 \geq C_1^0$, the equilibrium point corresponding to p^{*-} is stable, while the one corresponding to p^{*+} is always unstable.*

Proof. We will begin by proving the stability of the equilibrium state that makes biological sense. For this we will first see that $P(\lambda)$ has all its roots real and strictly negative, for which it is sufficient to show the result for $P_1(\lambda)$. In fact if we use the notation

$$\alpha = \mu_0 + \tau_{0\,1}\left(1 - \frac{a^{*-}}{C_1}\right),$$
$$\beta = \alpha 1\,2 + \tau_{0\,1}\frac{h^{*-}}{C_1},$$
$$\gamma_1 = \tau_{0\,1}^2\left(1 - \frac{a^{*-}}{C_1}\right)\frac{h^{*-}}{C_1},$$

then $P_1(\lambda)$ can be expressed in the form $\lambda^2 + (\alpha + \beta)\lambda + \alpha\beta - \gamma_1$, whose roots are

$$\lambda_{\pm} = \frac{-(\alpha + \beta) \pm \sqrt{(\alpha + \beta)^2 + 4\gamma_1}}{2}.$$

But from the fact that the equilibrium point makes biological sense, it follows that α, β and γ_1 are strictly positive, and so the roots of $P_1(\lambda)$ are strictly negative and different.

Note that these two roots depend on the value of C_1, and when $C_1 \to +\infty$ we have that $\alpha \to \mu_0 + \tau_{0\,1}$, $\beta \to +\tau_{1\,2}$ and $\gamma_1 \to 0$, and therefore $\lambda_- \to -\alpha_{0\,1}$ and

$\lambda_+ \to -\alpha_{1\,2}$. From this, it is concluded that, when $C_1 \to +\infty$, the polynomial $P(\lambda)$ converges uniformly to the polynomial

$$P_0(\lambda) = \prod_{r=0}^{5} (\lambda + \alpha_{r\,r+1})$$

on any compact subset of the complex plane. On the other hand, from the fact that

$$\frac{p^{*-}}{C_1} = \left(\varphi + \psi\frac{H}{C_1}\right) - \sqrt{\left(\frac{1}{K_a} - \psi\frac{H}{C_1}\right)^2 + \frac{\mu_0}{\tau_{0\,1}K_a}\left(\left(2 + \frac{\mu_0}{\tau_{0\,1}}\right)\frac{1}{K_a} + 2\psi\frac{H}{C_1}\right)}$$

and

$$\tau_{0\,1}\tau_{1\,2}\frac{h^{*-}}{C_1}$$
$$= \frac{\tau_{0\,1}\tau_{1\,2}}{2\mu_0\psi}\left(\psi\frac{H}{C_1} - \varphi + \sqrt{\left(\frac{1}{K_a} - \psi\frac{H}{C_1}\right)^2 + \frac{\mu_0}{\tau_{0\,1}K_a}\left(\left(2 + \frac{\mu_0}{\tau_{0\,1}}\right)\frac{1}{K_a} + 2\psi\frac{H}{C_1}\right)}\right)$$

converge to zero when $C_1 \to \infty$, we have that the polynomial $Q(\lambda)$ converges uniformly to the identically null polynomial over any compact set of the complex plane when $C_1 \to +\infty$. Using this result, it is easily proved that, for any simple closed curve Γ, strictly contained in the left half-plane of the complex plane and containing the roots of $P_0(\lambda)$ in its interior, we have that, for any sufficiently large value of the parameters C_1, the inequality

$$|Q(\lambda)| < |P(\lambda)|$$

is true for all $\lambda \in \Gamma$.

Then, from an application of Rouche's theorem (see [1, Ch. 5]), it follows that $P(\lambda)+Q(\lambda)$ also has all its roots in the interior of Γ and, therefore, the equilibrium state corresponding to p^{*-} will be stable for large values of the parameter C_1.

Let us now see that the equilibrium state corresponding to p^{*+} is unstable. Indeed, let us consider the equation for h in system (2.2), and substitute the term $\mu_0 h$ by $\mu_0 h^{*+}$ and $\left(1 - \frac{a}{C_1}\right)$ by $\left(1 - \frac{a^{*+}}{C_1}\right)$. It is easy to see that this equation has h^{*+} as equilibrium state and, for any initial condition h_0 different from h^{*+}, its solution

$$h(t) = h_0 e^{-\tau_{0\,1}\left(1 - \frac{a^{*+}}{C_1}\right)t} + \frac{H - \mu_0 h^{*+}}{\tau_{0\,1}\left(1 - \frac{a^{*+}}{C_1}\right)}\left(1 - e^{-\tau_{0\,1}\left(1 - \frac{a^{*+}}{C_1}\right)t}\right)$$

tends to infinity when $t \to +\infty$, because $h^{*+} > 0$ and $a^{*+} > C_1$. □

References

[1] L. V. Ahlfors, *Complex Analysis*, International Series in Pure and Applied Mathematics, McGraw-Hill, New York, 1978. MR 0510197.

[2] L. Alcalá, J. Quintero, C. González-Uribe, and H. Brochero, Productividad de *Aedes aegypti* (L.) (Diptera: Culicidae) en viviendas y espacios públicos en una ciudad endémica para dengue en Colombia, *Biomédica* **35** (2015) no. 2, 258–268. https://doi.org/10.7705/biomedica.v35i2.2567.

[3] P. Barbosa, T. M. Peters, and N. C. Greenough, Overcrowding of mosquito populations: responses of larval *Aedes aegypti* to stress, *Environ. Entomol.* **1** (1972), no. 1, 89–93. https://doi.org/10.1093/ee/1.1.89.

[4] R. Barrera, Simplified pupal surveys of *Aedes aegypti* (L.) for entomologic surveillance and dengue control, *Am. J. Trop. Med. Hyg.* **81** (2009), no. 1, 100–107. https://doi.org/10.4269/ajtmh.2009.81.100.

[5] R. Barrera, Control de los mosquitos vectores del dengue y del chikunguña: ¿es necesario reexaminar las estrategias actuales? *Biomédica* **35** (2015), no. 3, 297–299. https://revistabiomedica.org/index.php/biomedica/article/view/3053.

[6] M. A. Barrera-Pérez *et al.*, Control de criaderos de *Aedes aegypti* con el programa *Recicla por tu bienestar* en Mérida, México, *Salud Pública México* **57** (2015), no. 3, 201–210. https://www.saludpublica.mx/index.php/spm/article/view/7556.

[7] S. R. Christophers, *Aëdes Aegypti (L.): The Yellow Fever Mosquito: Its Life History, Bionomics and Structure*, Cambridge University Press, Cambridge, 1960.

[8] M. C. Domínguez, F. F. Ludueña Almeida, and W. R. Almirón, Population dynamics of *Aedes aegypti* (Diptera: Culicidae) in the city of Córdoba, *Rev. Soc. Entomol. Arg.* **59** (2000), no. 1-4, 41–50. https://www.biotaxa.org/RSEA/article/view/32372.

[9] *Dengue Guidelines for Diagnosis, Treatment, Prevention and Control*, New edition, WHO Press, Geneve, Switzerland, 2009. https://apps.who.int/iris/handle/10665/44188.

[10] Dengue vaccine: WHO position paper, July 2016 – recommendations, *Vaccine* **35** (2017), no. 9, 1200–1201. https://doi.org/10.1016/j.vaccine.2016.10.070.

[11] L. Esteva, G. Rivas, and H. M. Yang, Modelling parasitism and predation of mosquitoes by water mites, *J. Math. Biol.* **53** (2006), no. 4, 540–555. MR 2251788.

[12] I. Garcia da Silva, M. de Fátima Camargo, M. Elias, and C. N. Elias, Ciclo evolutivo de *Aedes (Stegomyia) aegypti* (Linnaeus, 1762) (Diptera, Culicidae), *Rev. Pat. Trop.* **22** (1993), no. 1, 43–48. https://revistas.ufg.br/iptsp/article/view/20069/.

[13] J. D. Gillett, E. A. Roman, and V. Phillips, Erratic hatching in *aedes* eggs: a new interpretation, *Proc. R. Soc. Lond. B.* **196** (1977), no. 1123, 223–232. https://doi.org/10.1098/rspb.1977.0038.

[14] T. P. Herrera-Ramírez, *Modelación matemática de la dinámica de los estadios inmaduros del* Aedes aegypti *en un criadero*, Tesis (Doctorado), Benémerita Universidad Autónoma de Puebla, Puebla, 2021. https://hdl.handle.net/20.500.12371/16447.

[15] S. Ibáñez-Bernal and H. Gómez-Dantés, Los vectores del dengue en México: una revisión crítica, *Salud Públ. Méx.* **37** (1995), suppl., S53–S63.

[16] T. P. Livdahl, R. K. Koenekoop, and S. G. Futterweit, The complex hatching response of *Aedes* eggs to larval density, *Ecol. Entomol.* **9** (1984) no. 4, 437–442. https://doi.org/10.1111/j.1365-2311.1984.tb00841.x.

[17] P. Manrique-Saide, H. Delfín-González, V. Parra-Tabla, and S. Ibáñez-Bernal, Desarrollo, mortalidad y sobrevivencia de las etapas inmaduras de *Aedes aegypti* (Diptera: Culicidae) en neumáticos, *Rev. Biomed.* **9** (1998), no. 2, 84–91. https://www.imbiomed.com.mx/articulo.php?id=20252.

[18] M. B. Nathan, D. A. Focks, and A. Kroeger, Pupal/demographic surveys to inform dengue-vector control, *Ann. Trop. Med. & Parasitol.* **100** (2006), suppl. no. 1, 1–3. https://doi.org/10.1179/136485906X105462.

[19] M. J. Nelson, *Aedes Aegypti: Biology and Ecology*, General Publications, PAHO, Washington, D.C., 1986. https://iris.paho.org/handle/10665.2/28514.

[20] Organisation for Economic Co-operation and Development (OECD), *Safety Assessment of Transgenic Organisms in the Environment, Volume 8: OECD Consensus Document of the Biology of Mosquito* Aedes Aegypti, Harmonisation of Regulatory Oversight in Biotechnology, OECD Publishing, Paris, 2018. https://doi.org/10.1787/9789264302235-en.

[21] Organización Panamericana de la Salud. *Documento Técnico para la Implementación de Intervenciones Basado en Escenarios Operativos Genéricos para el Control del* Aedes aegypti, OPS, Washington, D.C., 2019. https://iris.paho.org/handle/10665.2/51654.

[22] E. Pliego-Pliego, O. Vasilieva, J. Velázquez-Castro, and A. Fraguela Collar, Control strategies for a population dynamics model of *Aedes aegypti* with seasonal variability and their effects on dengue incidence, *Appl. Math. Model.* **81** (2020), 296–319. MR 4050781.

[23] J. R. Powell, Mosquito-borne human viral diseases: why *Aedes aegypti*? *Am. J. Trop. Med. Hyg.* **98** (2018), no. 6, 1563–1565. https://doi.org/10.4269/ajtmh.17-0866.

[24] J. A. Quesada Aguilera, E. Quesada Aguilera, and N. Rodríguez Socarras, Diferentes enfoques para la estratificación epidemiológica del dengue, *Arch. Méd. Camagüey* **16** (2012), no. 1, 109–123. http://scielo.sld.cu/scielo.php?script=sci_abstract&pid=S1025-02552012000100014.

[25] E. Quispe, A. Carbajal, J. Gozzer, and B. Moreno, Ciclo biológico y tabla de vida de *Aedes aegypti*, en laboratorio: Trujillo (Perú), 2014, *Rebiolest* **3** (2015), no. 1, 91–101.

[26] A. C. Ramos and R. A. Prado Castillo, *Efecto que tienen las campañas de prevención y educación sobre el control de vector del dengue* Aedes aegypti *en la ciudad de León*, Tesis (Licenciatura), Universidad Nacional Autónoma de Nicaragua, León, 2012. http://riul.unanleon.edu.ni:8080/jspui/handle/123456789/5719.

[27] M. R. Silva, P. H. G. Lugão, and G. Chapiro, Modeling and simulation of the spatial population dynamics of the *Aedes aegypti* mosquito with an insecticide application, *Parasites Vectors* **13** (2020), article no. 550. https://doi.org/10.1186/s13071-020-04426-2.

[28] V. C. Soares-Pinheiro, W. Dasso-Pinheiro, J. M. Trindade-Bezerra, and W. P. Tadei, Eggs viability of *Aedes aegypti* Linnaeus (Diptera, Culicidae) under different environmental and storage conditions in Manaus, Amazonas, Brazil, *Braz. J. Biol.* **77** (2017), no. 2, 396–401. https://doi.org/10.1590/1519-6984.19815.

[29] H. M. Yang, M. L. G. Macoris, K. C. Galvani, and M. T. Macoris Andrighetti, Follow up estimation of *Aedes aegypti* entomological parameters and mathematical modellings, *Biosystems* **103** (2011), no. 3, 360–371. https://doi.org/10.1016/j.biosystems.2010.11.002.

T. Herrera-Ramírez
Facultad de Ciencias Físico Matemáticas, Benemérita Universidad Autónoma de Puebla, Mexico
tishbe.herrera@alumno.buap.mx

A. Fraguela-Collar✉
Facultad de Ciencias Físico Matemáticas, Benemérita Universidad Autónoma de Puebla, Mexico
fraguela@fcfm.buap.mx

J. Velázquez-Castro
Facultad de Ciencias Físico Matemáticas, Benemérita Universidad Autónoma de Puebla, Mexico
jorge.velazquezcastro@correo.buap.mx

C. A. Abella-Medrano
Facultad de Ciencias Físico Matemáticas, Benemérita Universidad Autónoma de Puebla, Mexico
abella22@gmail.com

Received: June 12, 2021
Accepted: September 12, 2021